AD-A031 330 TEXACO INC BEACON N Y TEXACO RESEARCH CENTER F/G 21/7
A PERFORMANCE MODEL FOR THE TEXACO CONTROLLED COMBUSTION, STRAT--ETC(U)
JAN 76 B C JAIN, J C KECK, J M RIFE DAAE07-73-C-0282

UNCLASSIFIED NL

1 OF 1
ADA031330

END
DATE
FILMED
12 - 76

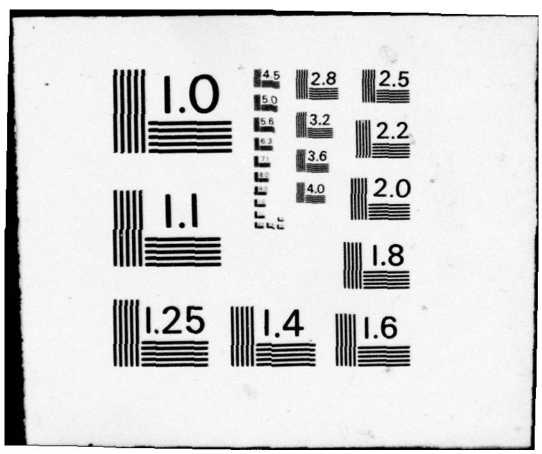
1.0
4.5
5.0
5.6
6.3
2.8
3.2
3.6
4.0
2.5
2.2
2.0
1.1
1.8
1.25
1.4
1.6

Fluid Mechanics Laboratory
Publications No. 76-2

A PERFORMANCE MODEL FOR THE TEXACO CONTROLLED COMBUSTION STRATIFIED CHARGE ENGINE

Bhag C. Jain, James C. Keck, and Joe M. Rife

January 1976

FLUID MECHANICS LABORATORY

DEPARTMENT OF MECHANICAL ENGINEERING
MASSACHUSETTS INSTITUTE OF TECHNOLOGY

2

6

A PERFORMANCE MODEL FOR THE TEXACO CONTROLLED COMBUSTION, STRATIFIED CHARGE ENGINE,

15 DAAE07-73-C-0282, DAAE07-74-C-0268

by

10

Bhag C. Jain, James C. Keck, ~~and~~ Joe M. Rife

Fluid Mechanics Laboratory
Department of Mechanical Engineering
Massachusetts Institute of Technology

11 January 1976

12 53p.

Technical and financial support for this research was provided by U.S. Army-Tank Automotive Systems Development Center (Prov) by subcontract to M.I.T. from Texaco, Inc., under contracts No. DAAE07-73-NEW C-0282, DAAE07-74-C-0268, and DAAE07-74-C-0168.

plus 0168 contract

347300

A PERFORMANCE MODEL FOR THE TEXACO CONTROLLED

COMBUSTION, STRATIFIED CHARGE ENGINE

Bhag C. Jain, James C. Keck, and Joe M. Rife
Department of Mechanical Engineering
Massachusetts Institute of Technology
Cambridge, Massachusetts 02139

A

ABSTRACT

A model has been developed to predict the performance of the Texaco Controlled Combustion, Stratified Charge Engine starting from engine geometry, fuel characteristics and the operation conditions. This performance model divides the engine cycle into the following phases: Intake, Compression, Rapid Combustion, Mixing - Dominated Expansion, Heat - Transfer Dominated Expansion and Exhaust. During the rapid combustion phase, the rate of heat release is assumed to be controlled by the rate of fuel injection and the gas-to-fuel ratio. Entrainment of the surrounding gas by the plume is assumed to be controlled by the turbulent eddy entrainment velocity.

A plume geometry model has been developed to obtain the surface area of the plume for entrainment during the mixing dominated phase. The model also gives the wall areas in contact with the hot, burned gas plume and the relatively cold unburned gas for heat transfer calculations.

Comparison of the model predictions with the available experimental data shows good agreement. In addition, the potential of the performance model as a design tool is demonstrated with a parametric analysis.

-A-

I. INTRODUCTION

The term stratified charge engine is generally accepted to describe a spark-ignition, internal combustion engine with a non-uniform fuel-air mixture in the combustion chamber. With the increased emphasis on the exhaust emissions and fuel economy over the past few years; interest in the stratified charge engine has risen dramatically and various approaches for stratification of the fuel-air mixture have been studied in depth. In this paper, we discuss a performance model for the Texaco direct injection stratified charge engine. The Texaco Controlled Combustion System (TCCS) demonstrates excellent fuel economy, broad fuel tolerance and relatively low emissions.
The basic conceptual details behind the Texaco Controlled Combustion System are described below and additional details can be found in the references on the TCCS engine (1-4).

TCCS Engine Description

The Texaco Controlled Combustion System is illustrated schematically in Figure 1. A high air swirl is induced by the flow through the inlet valve and is amplified during compression by the combustion chamber configuration. The combustion chamber is a cup in the piston with a cylindrical upper section and toroidal bottom. The diameter of the cup is approximately one half of the cylinder diameter.

The high pressure injection system is based on diesel engine components and uses a special version of the standard Roosa Master Pencil Nozzle. The distinguishing feature of this nozzle is a flat seat and a single-hole orifice instead of the more usual conical seating, multiple-hole sac-tip design. All of the remaining details are essentially equivalent to the standard production nozzle. Valve opening pressure is typically set at 1500-2000 psi. The ignition system developed for the engine, referred to as The Texaco Ignition System (TTIS), is a high energy, multi-discharge unit with controlled duration (5).

High pressure injection of the fuel into the swirling air in a downstream direction begins near the end of the compression stroke. The first increment of fuel is ignited as it reaches the spark plug and a flame-front is established immediately downstream of the spark plug. As fuel injection continues, additional fuel and air reach the flame front at the spark plug and the fuel is burned almost as rapidly as it is injected. In full load operation the fuel injection interval corresponds approximately to the time for one air swirl and the overall air-fuel ratio is near stoichiometric. Lower loads are obtained by decreased fuel injection duration and quantity, consequently the overall air-fuel ratio is lean and may approach 100:1 at idle conditions.

Typical diesel engine problems of long igniton delay, high rates of pressure rise and high peak pressures with low cetane fuels and low compression ratio are avoided in TCCS operation by providing positive ignition source. The problems of spontaneous ignition and octane requirement associated with conventional gasoline engines are also eliminated with TCCS since the residence time of combustible fuel-air mixtures is extremely short.

In summary, the TCCS mode of operation results in several unique characteristics including high part-load thermal efficiency at lean mixtures and inherently low hydrocarbon and carbon monoxide emissions resulting from excess air operation and controlled combustion rates. In addition, with the high pressure injection system, a wide range of fuel volatility can be tolerated with no apparent sensitivity to either the octane or cetane number of the fuel. These characteristics, in addition to quick warm-up and excellent driveability are significant factors in achieving an automotive engine with the potential for good performance and low exhaust emissions.

The purpose of the research work to be described in the following pages has been to develop a model to predict the performance of the TCCS, stratified charge engine given the engine geometry, operating parameters and the fuel properties. Once the model is shown to be effective in predicting the performance, it can then be used as a design tool. With the brief description of the geometry and the mode of operation of the engine given above, we will now proceed to a discussion of the model.

II. THE MODEL

Basis for the Model Development

A set of performance data including pressure-volume diagrams was supplied by Texaco at the beginning of our research program. The data was obtained on an engine having a different geometry (a hemispherical combustion chamber rather than the cup-in-the-piston); however, the engine used the basic TCCS concept and it was felt that an analysis of this data would give some insight into the working of the engine. Data, for various speeds, loads and fuels, was plotted in the form of PV^γ plots. Because PV^γ is constant for an isentropic process and changes only due to real effects (which are small), an examination of the value of PV^γ just before, during and after combustion gives a very good idea of the net heat input or output to the working fluid due to heat release as a result of chemical reaction and/or heat losses.

Some typical PV^γ plots are shown in Figures 2 and 3. Figure 2 is for 1200 RPM full load case with three different fuels - gasoline, JP-4 and diesel and Figure 3 is for 1200 RPM with two different load conditions with gasoline as the fuel. In generating these plots, the cylinder pressure and volume at start of injection have been used as the reference (P_o,V_o). The value of the specific heat ratio γ before start of combustion corresponds to that for unburned gas mixtures while the value of γ during and after combustion corresponds to that for burned gas mixtures at the overall equivalence ratio. While this will not be strictly correct - especially during combustion when γ changes from the value for unburned mixture to that of the burned gas mixture - the error introduced is small since combustion is rapid and takes place near top dead center. The ratio of volumes (V/V_o), thus, is close to one. Since the purpose of this analysis has been to obtain a qualitative understanding of the processes taking place, a slight error in the value of γ can be tolerated.

Some general conclusions can be drawn on the basis of this analysis. The value of PV^γ starts to rise sharply a few crankangle degrees after the start of injection. The duration of this steep rise in the value of PV^γ appears to correspond to the duration of injection. This suggests that the fuel burns as soon as it reaches the vicinity of the spark plug and the delay between the start of injection and the start of the rapid rise in the value of PV^γ can be associated with the jet transit time from the nozzle to the spark plug. The slower rise in the value of PV^γ that follows this steep rise appears to be mixing controlled. The fact that PV^γ starts to drop later in the cycle suggests that as mixing nears completion, heat losses to the engine walls dominate. Another interesting conclusion is that there appears to be no substantial difference in the general nature of these plots for the different fuels considered here. It must be noted that the total chemical energy input, that is the mass injected times the lower heating value of the fuel, was also approximately the same for all three fuels.

In addition to the performance data, a high speed movie of the combustion process inside the engine cylinder was also supplied by Texaco. The combustion movie showed that first increments of the fuel to be injected took a few crankangle degrees to reach the spark plug and that as soon as they reached the spark plug, these increments were ignited. This observation confirmed the conclusion derived from analyzing the PV^{γ} plots.

The information obtained from the analysis of the pressure-volume data, the combustion movie and from the literature on the development of the TCCS concept was used as the basis for a simplified theoretical model to predict the performance of the engine.

The Performance Model: Qualitative Description

The model divides the complete engine cycle into the following phases: intake, compression, rapid combustion, mixing dominated expansion, heat transfer dominated expansion and exhaust. It assumes that rapid combustion follows the injection process with a time delay equal to the jet transit time. The delay period is treated as part of the compression phase and the presence of the small quantities of injected fuel is neglected for the analysis. The rate of heat release during the rapid combustion phase is determined by the rate of fuel injection and the rate of entrainment of air by the fuel spray. The entrainment of the air is treated by assuming that rapid combustion occurs at a fixed combustion equivalence ratio determined by an analysis of the process of spray formation and air entrainment. This analysis of the process of spray formation and entrainment of air by the fuel jet is treated by a jet mixing analysis[6]. Of course, in reality, combustion takes place at a wide range of equivalence ratios across the jet but the net effective heat release rate for the purpose of performance modelling can be assumed to take place at the mean equivalence ratio determined by the analysis mentioned above.

During the rapid combustion and the mixing dominated phases, the charge inside the cylinder will consist of a plume of hot burned gas surrounded by an unburned gas mixture. We observe from the combustion movies that the plume starts at the spark plug and is swept around by the air motion in the combustion chamber. Figure 4 qualitatively shows the initial stages of the hot burned gas plume. The sectional view shown in Figure 4 is taken through the cylinder axis and spark location. In the initial stages, the plume can be considered to be a section of a torus. As more and more fuel is injected and burned, the hot burned gas plume closes on itself forming a complete torus. The geometry of the plume is modified as it grows larger as discussed in Appendix I. Once the mixing process is complete, the charge inside the cylinder consists of burned gas alone and the plume occupies the total cylinder volume. Thus, during the rapid combustion and the mixing dominated phases, the total wall area for heat transfer can be divided into two parts - one in contact with the hot, burned gas plume and the other in contact with the relatively cold, unburned gas. The plume geometry model, described in Appendix I, is then used to obtain the two areas for heat transfer during these phases.

A better understanding, of the various phases introduced in the model, can be obtained by referring to PV^{γ} plots, as shown in Figure 5. Let us first consider a hypothetical case where there is no heat transfer to or from the working fluid and where intake and exhaust processes have not been included. In this case, the value of PV^{γ} remains constant during compression and towards the end of the compression phase; fuel injection begins. The delay period, before the start of the rapid combustion, is treated as part of the compression phase and the presence of small quantities of fuel is ignored. During the rapid combustion phase, the value of PV^{γ} rises rapidly and the rate of rise is determined by mass rate of injection and the assumed combustion equivalence ratio. At this point in the cycle, we have a plume of hot burned gas surrounded by relatively cold air. As the plume entrains surrounding air, additional chemical heat release and/or the mixing of hot and cold gases with different heat capacities results in an additional, though slower, rise in the value of PV^{γ}. This is the mixing dominated part of the expansion phase and it ends when all of the air is "consumed" by the hot burned gas plume. Now the whole charge consists of the burned gas at the overall fuel-air ratio for the cycle and as we have assumed no heat transfer to or from the working fluid, the value of PV^{γ} remains constant until the exhaust valve opens. The effect of heat transfer can now be put in qualitatively - a heat loss from the working fluid lowers the value of PV^{γ} as shown by the solid curve in Figure 5. With this qualitative description of the various phases, we now proceed to a detailed, quantitative treatment of each of the phases and, thereby, of the complete cycle.

The Performance Model: Quantitative Description

Before giving a description of the individual phases, we will discuss some aspects of the model which are common for all phases. These include treatment of gas properties - both unburned and burned gas and the treatment of heat transfer in general.

Gas Properties: For air, heat capacities have been treated as functions of temperature alone. The burned gas properties have been treated on the basis of some approximate relationships developed by Michael K. Martin (7) at the Sloan Automotive Laboratory. These approximate relationships have been checked against a thermodynamic equilibrium program involving some 46 different species with agreement to $\pm$ 3% over the range of interest.

Heat Transfer Correlation: Heat transfer has been treated largely with a technique based on Woschni's universal correlation[8]. The gas velocities have been modified to include the effect of high swirl which is assumed to be additive. The swirl is treated as solid body rotation near top dead center where most of the events of interest occur.and the velocities due to swirl dominate. Heat transfer areas are divided into two parts and the heat transfer coefficient for each part is calculated separately. The total heat transfer is obtained by summing the contributions of each of the parts (see Appendix I).

We will now begin with a detailed description of the compression phase. Assumptions for each of the phases will be explicitly noted and the equations used for predicting pressure and other performance parameters will be described. The gas properties and the heat transfer are treated as noted above.

Compression Phase: During the compression phase, the charge is considered to be a homogeneous mixture of air, residual gas and the exhaust gas recirculated (EGR). This mixture will from now on, be referred to as the "unburned gas mixture". As stated earlier, the presence of the small quantity of fuel during the ignition delay period will be neglected. With these assumptions, we can write down the equation of state and mass and energy conservation equations as follows:

Equation of state

$$PV = m_u R_u T \qquad (1)^*$$

---

*See list of symbols for definition of the terms in the equations.

Mass conservation

$$m_u = (m_u)_o \text{ or } v_u = \frac{V}{m_u}$$

Energy conservation

$$E\text{-}W\text{-}Q = m_u e_u \tag{2}$$

where work done $W = \int PdV$, and,

$$(m_u)_o = (m_A)_o + m_{RG} + m_{EGR} \tag{3}$$

$(m_A)_o$, m_{RG} and m_{EGR} are the masses of air, residual gas and recirculated exhaust gas at the end of intake stroke. The recirculated and residual exhaust gas fractions are defined as follows:

$$EGR = m_{EGR} / [(m_A)_o + m_{EGR}] \tag{4}$$

$$RG = m_{RG} / [(m_A)_o + m_{EGR} + m_{RG}] \tag{5}$$

so that

$$m_{EGR} = (EGR)*(m_A)_o / (1-EGR) \tag{6}$$

$$m_{RG} = (RG)*[(m_A)_o + m_{EGR}]/(1-RG) \tag{7}$$

It is assumed that residual gas and the recirculated exhaust gas are burned gases at the overall equivalence ratio. Gas properties for the burned gases and air as well as the heat transfer Q are obtained from the analyses described in previous section of this paper. Equations (3), (6), and (7) with gas properties are used to determine the right-hand side of equation (2) and these equations can be used to predict the pressure. As both W and Q involve pressure (P) and/or temperature (T) in their evaluation, a simple iterative scheme is used.

Rapid Combustion Phase: The rapid combustion phase is assumed to follow fuel injection after the jet transit time delay. As previously described we assume that rapid combustion takes place at a constant combustion equivalence ratio for the purpose of performance modelling. Once the unburned gas entrained by the fuel jet as it reaches the spark plug is known from the spray analysis (6), the combustion equivalence ratio (ϕ_c) can be determined as follows:

Let the ratio of the mass of unburned gas entrained to the mass of fuel at the spark plug be $(G-F)_{sp}$. The fraction of air in a unit mass of unburned gas mixture is:

$$\frac{(m_A)_o}{(m_u)_o} \tag{8}$$

The combustion equivalence ratio (ϕ_c) then is:

$$\phi_c = \frac{(m_u)_o}{(m_A)_o *(G-F)_{s-p} *F_c} \tag{9}$$

where F_c is the chemically correct fuel-air ratio.

Because the gas mixture entrained in the burned gas plume contains residual gas and air, the equivalence ratio of hot burned gas plume is different than ϕ_c. This equivalence ratio ϕ can be calculated if it is assumed that the residual gas and the exhaust gas recirculated are burned gases at the overall equivalence ratio ϕ_o.

The charge inside the cylinder can then be considered as consisting of a plume of hot burned gas at the equivalence ratio, ϕ, and the unburned gas mixture outside the plume. The equations of state and mass and energy conservation can then be written as follows:

Equations of State

Unburned gas mixture

$$PV_u = m_u R_u T_u \tag{10}$$

Burned gas

$$PV_b = m_b R_b T_b$$

Mass conservation:

$$m_u + m_b = (m_u)_o \tag{11}$$

Energy conservation:

$$E\text{-}W\text{-}Q = m_u e_u + m_b e_b \tag{12}$$

Also, note that $V_u + V_b = V$

The work, W, heat transfer, Q, and gas properties are treated as described earlier. Of course, the heat transfer now must be divided into two parts due to the presence of the hot, burned gas plume.

These equations have again been solved using a simple, iterative scheme to predict cylinder pressure and other performance parameters as a function of time (crank-angle degrees) during the rapid combustion phase. The rapid combustion phase ends when all the injected fuel has reached the spark plug.

Expansion Phase: This phase starts at the end of the rapid combustion phase and continues until the exhaust valve starts to open when blowdown and the exhaust phase take over. This phase has been divided into two parts, a mixing dominated phase and a heat transfer dominated phase.

(a) Mixing Dominated Expansion Phase: At the beginning of this phase, the charge inside the cylinder is considered to consist of a hot, burned gas plume surrounded by a relatively cold unburned gas mixture. The plume slowly entrains this surrounding gas and as it does so, it is assumed that the entrained gas is perfectly mixed throughout the plume resulting in a new equivalence ratio for the plume at any instant. This entrainment and mixing also results in some chemical heat release due to combustion if the plume is initially richer than stoichiometric.

The entrainment of the surrounding gas mixture by the plume has been treated following the work of Blizard and Keck (9) which relates the turbulent eddy entrainment velocity to the engine inlet speed. The surface area of the plume for entrainment of the surrounding gas mixture is obtained from the plume geometry model (Appendix I). Thus the mass rate of entrainment of surrounding gas mixture can be given as

$$\dot{m}_e = S_e U_e \sqrt{\rho_u \rho_b} \qquad (13)$$

Where the plume area S_e at any instant is given by the plume geometry model and the turbulent eddy entrainment velocity, U_e, is taken from Blizard and Keck:

$$U_e \simeq 0.28\, U_i$$

and

$$U_i = \varepsilon_v (b^2/2DL) NS \qquad (14)$$

Knowing the mass rate of entrainment, the fractions of the constituents of the entrained gas mixture and the old equivalence ratio of the plume; the new equivalence ratio for the plume is calculated. Thus the charge in the cylinder during this phase can be treated exactly like that during the rapid combustion phase except that the equivalence ratio of the plume now changes;in contrast to a constant combustion equivalence ratio during the entire rapid combustion phase. The varying equivalence ratio is taken into consideration when evaluating the plume gas properties. Since the rest of the treatment is exactly similar to that during the rapid combustion phase, the equations of state and mass and energy conservation will not be repeated here.

The mixing dominated phase persists until all of the unburned gas mixture has been entrained; or, if mixing is not complete, until the exhaust valve starts to open. In the latter case, there is no heat-transfer dominated phase and at the start of blow-down the mixing dominated phase is terminated. The composition is frozen and mean gas properties overall are defined. If, on the other hand, mixing is complete before the exhaust valve starts to open, it is followed by the heat transfer-dominated expansion phase.

<u>Heat Transfer Dominated Expansion Phase</u>: At the beginning of this phase, the charge inside the cylinder is considered to be homogeneous burned gas at the overall equivalence ratio as the mixing is now complete. The treatment, then,is similar to that for the compression phase except that the charge is burned rather than unburned gas. The only important process going on is the heat transfer to the

walls. The equations, replacing subscript 'u' by subscript 'b' for those of the compression phase are

Equation of state:

$$PV = m_b R_b T$$

Mass conservation:

$$m_b = (m_u)_o \text{ Or } v_b = \frac{V}{m_b}$$

Energy conservation:

$$E-W-Q = m_b e_b$$

and the performance is predicted in a manner similar to that in the compression phase. This phase ends when the exhaust valve starts to open.

<u>Exhaust and Intake Phases</u>: The mass flow rates through exhaust and intake valves have been treated as quasi-steady flow through a restriction. The governing equations can be written as follows:

$$\dot{m} = C_v A_v \left(\frac{RT_o}{P_o}\right) (\gamma RT_o)^{1/2} \left\{(2/(\gamma-1))\left[\left(\frac{P_2}{P_o}\right)^{2/\gamma} - \left(\frac{P_2}{P_o}\right)^{(\gamma+1)/2(\gamma-1)}\right]\right\}^{1/2} \quad (15)$$

for subsonic flow, and

$$\dot{m} = C_v A_v \left(\frac{P_{oc}}{RT_{oc}}\right) (\gamma RT_o)^{1/2} \left\{\left[\frac{2}{(\gamma+1)}\right]^{(\gamma+1)/2(\gamma-1)}\right\}^{1/2} \quad (16)$$

for choked flow, with the condition for choked flow being:

$$\frac{P_o}{P_s} > \left(\frac{\gamma+1}{2}\right)^{\gamma/(\gamma-1)} \quad (17)$$

where C_v = valve discharge coefficient

A_v = valve flow area

P_o, T_o are upstream stagnation pressure and temperature,

P_2 = downstream static pressure

and P_{oc}, T_{oc} are stagnation pressure and temperature for choked flow. The flow through exhaust and intake valves is treated with these equations and the logic to take care of the reverse flows through the valves has been put into the computer program. Before these equations can be used to obtain the mass rates of flow, a knowledge of discharge coefficients and valve flow areas is required both for exhaust and intake valves. This information has been obtained from the data supplied by Texaco.

In addition to the flow equations, equations of state, mass and energy conservation are used to model the exhaust and the intake phases. The equations of state and mass conservation are:

$$PV = mRT \tag{18a}$$

$$m = (m_u)_o + m_{in} - m_{ex} \tag{18b}$$

The energy equation for an open system, after some mathematical manipulation and use of equation of state, can be written as follows

$$\frac{\dot{T}}{T} = \frac{R}{C_p - R}\left[\frac{-\dot{Q} + (\dot{m}_{in}h_{in} - \dot{m}_{ex}h_{ex} - \dot{m}h)}{mRT} - \frac{\dot{MW}}{MW} + \frac{\dot{V}}{V} - \frac{\dot{m}}{m}\right] \tag{19}$$

The energy equation (19) along with the flow equations (16 or 17) and the equations for heat transfer and work form a set of simultaneous linear differential equations. These have been solved numerically using the fourth order Runga-Kutta method resulting in the predictions for the exhaust and intake phases.

Thus the performance modelling of the cycle is complete. In addition to the detailed performance predictions made during each of the phases, the overall engine performance parameters can also be obtained. The predictions for the motored engine can also be obtained from the complete model by removing rapid combustion and mixing dominated phases leaving the intake, compression, expansion, and exhaust phases.

A number of computer programs have been developed to carry out the steps described in the model and give as outputs, overall performance, detailed performance and plots of cylinder pressure and PV^{γ} as functions of crank-angle.

The model, as described, requires an input from the spray analysis; specifically, the entrained gas to fuel ratio at the spark plug. In addition, we have not explicitly discussed the multi-fuel capability of the engine and have not indicated the limitations of the model as with regard to type of fuels for which the model can be used. These questions appear to be more properly addressed in the spray analysis (6).

III PREDICTIONS OF THE MODEL

Comparison with Experimental Data:

A 3 7/8" x 3 7/8" single cylinder engine designed by Texaco has been set up at the Sloan Automotive Laboratory at MIT to carry out experimental investigations on TCCS, stratified charge concept. A CFR 48 crankcase has been modified to accept a cylinder sleeve assembly, head, crankshaft, piston and valve train assembly supplied by Texaco.

In addition to the preliminary data obtained with the single cylinder engine set up at the Sloan Automotive Laboratory, similar data has been supplied by Texaco. The performance model has been used in conjunction with the gas-to-fuel ratio supplied by the jet model (6) to predict engine performance starting from the engine geometry, operating conditions and fuel properties. The predictions have then been compared with the available engine data from Texaco as shown in Figures (6) and (7). The fuel used at Texaco was gasoline and injection timing was set at 28° BTC for 2500 RPM and at 20° BTC for 1500 RPM at full loads. Ignition timing was matched to the start of injection at full loads. As shown in Figures (6) and (7) the predictions of the model agreed well with the experimental data obtained from single cylinder engine set ups.

The performance model can also be used in conjunction with the jet model (6) to predict the effects on the performance of the engine if any of the input parameters are changed. The models, therefore, have a potential to be used as design tools.

Predictions of the Performance Model and Its Uses as a Design Tool:

A parametric study has been carried out with the performance model to demonstrate this potential as a design tool. The various parameters considered are the fraction of the exhaust gas re-circulated (EGR), injection timing, gas-to-fuel ratio at the spark plug and the duration of injection. The calculations, changing one of these parameters at a time, have been carried out for 2500 RPM engine speed and 3/4 of the full load fuel injection. All parameters are held at their present design values except the single parameter to be considered. The present design values as well as the range of parameters used in this study have been listed in Table 1.

The effects of these changes on performance as predicted by the model are shown in Figures (8) through (12). In each of these figures, the top box shows the net work done, heat loss and the energy of the exhaust gas as a fraction of the total chemical energy of the injected fuel. Below it are the indicated mean effective pressure and the blowdown temperature defined as the temperature of the exhaust gas at the beginning of blowdown. Because the amount of total fuel injected is fixed for all the cases to be described, the curve for indicated mean effective pressure is also a measure of the inverse indicated specific fuel consumption. A dotted vertical line shows the present design and operating conditions in all figures.

Figure (8) shows the effect of various fractions of EGR on the performance as predicted by the performance model. As the exhaust gas recirculated increases, the indicated mean effective pressure and thereby the power putput goes down. Looking at the energy balance we see that the heat loss also goes down whereas the energy of the exhaust gases increases to compensate for the other two. Of course, because of the excess air operation of the engine for part loads, the loss in power output is not quite as dramatic as it would be at full load where any amount of EGR will result in a reduction in the amount of air available for combustion.

The effect of changing the start of injection is shown in Figure (9). As far as the power output and fuel consumption are concerned, the present timing is very close to optimal as expected from performance data. Both advancing as well as retarding the injection from its present value adversely affect the power output. As can also be seen from the figure, the energy of the exhaust as well as the blowdown temperature rise as injection is retarded. The peak pressure in the cycle is found to vary from 30 atmospheres to almost 60 atmospheres as the injection timing is varied with peak pressure rising as the injection timing is advanced.

Figure (10) shows the effect of a change in the gas-to-fuel ratio at the spark plug. There are many ways in which this ratio can be changed by changing injection parameters (6). While the other two parameters discussed so far - EGR and the injection timing can be classified as operating conditions easily amenable to change, a change in the gas-to-fuel ratio at the spark plug requires basic design changes - a change in the distance between nozzle tip and the spark plug, modified swirl rates or a change in the injection system such as orifice size or angle of injection. As can be seen from Figure (10), any reduction in gas-to-fuel ratio from the present value will adversely affect the performance. This is to be expected because a lower gas-to-fuel ratio means that less of the total chemical energy is released during "rapid combustion" and more and more is released during the slower, mixing-dominated phase of the expansion stroke. As the gas-to-fuel ratio is farther reduced, the mixing may not be complete as the exhaust valve opens. As more and more chemical energy is released later in the expansion phase, the energy in the exhaust and its temperature go up. An increase in gas-to-fuel ratio at the plug, on the other hand, increases the power output - but only marginally and as we reach stoichiometric mixtures at the spark plug, the indicated mean effective pressure curve flattens out. Considering that the gain in performance is only marginal if the ratio is increased, any design changes to bring about this increase would have to be carefully scrutinized. There may be some considerations - other than the power output - which may weigh in favor of a less rich or even slightly lean rapid combustion phase; including reduction in soot and oxides of nitrogen. The peak pressures in the cycle rise to nearly 63 atmospheres as the rapid combustion appreaches stoichiometric gas-to-fuel ratios.

Figure (11) shows a typical set of PV^{γ} plots obtained from the parametric study. The case shown here is the variation of gas-to-fuel ratio at the spark plug and these plots very clearly show that as the gas-to-fuel ratio at the spark plug is increased, more and more heat is released during the rapid combustion phase.

The last parameter considered here is the duration of injection. The predictions for such a case as shown in Figure (12). The injection is assumed to be a square wave pluse. The injection timing is assumed to be such that the start and end of the rapid combustion are symmetrical about top dead center. As we see from the figure, there is a small gain in the power output as the injection duration is reduced. Of course, the rates of pressure rise go higher and higher as the duration is reduced - cylinder pressure rising from 22 to 55 atmospheres in 10 crank-angle degress for the extreme case considered here.

Clearly, these are but a few examples where the model can be used to predict the effect on the engine performance of any proposed changes in the design and/or operating conditions of the engine. The purpose here has been to bring out the potential application of the model as a design tool rather than to provide an exhaustive mapping of all possible changes.

IV CONCLUSIONS AND DISCUSSION

(i) A performance model for the Texaco Controlled Combustion, Stratified Charge Engine has been developed to predict engine performance starting from engine geometry, fuel characteristics and the operating conditions.

(ii) Parametric analysis has been carried out using the performance model to illustrate its potential use as a design tool.

(iii) The model can be used as a basis for models to predict emission characteristics of the engine. For this purpose, the assumptions of rapid combustion at a mean equivalence ratio and complete mixing within the plume will have to be modified. While predicting emissions has not been a purpose of the model so far, some qualitative observations can be made. The transition of the hot, burned gases from the rich rapid combustion products to leaner mixtures is controlled by the mixing and is rather slow. This may result in significant nitric oxide formation. The unburned hydrocarbons may be largely formed at the outer bounds of the spray at very lean mixtures and also from the tail end of the injection pulse if the cut-off is not sharp. The model, with suitable modifications, should be useful in predicting emission characteristics of the engine.

The authors are thankful to Professors Heywood and Hoult of M.I.T., Mr. Ed Mayer of Texaco and Mr. Walter Bryzik of USATACOM for their help in this work. Technical and financial support for this research was provided by U.S. Army-Tank Automotive Systems Development Center (Prov) by subcontract to M.I.T. from Texaco, Inc., under contracts No. DAAE07-73-C-0282, DAAE07-74-C-0268, and DAAE07-74-C-0168.

REFERENCES

1. Davis et. al., "Fuel Injection and Positive Ignition - A Basis for Improved Efficiency and Economy." Paper 190A presented at SAE Summer Meeting, Chicago, June, 1960.

2. Mitchell, et al., "Design and Evaluation of a Stratified Charge Multifuel Military Engine." SAE Transactions, Vol. 77 (1968), Paper 680042.

3. Mitchell eat al., "A Stratified Charge Multifuel Military Engine - A Progress Report." SAE Paper 720051.

4. Alperstein et al., "Texaco's Stratified Charge Engine - Multifuel, Efficient, Clean and Practical." SAE Paper 740563.

5. Canup, R.E.,"The Texaco Ignition System - A New Concept for Automotive Engine." SAE Paper 750347.

6. Jain et al.,"A Model for Fuel-Air Mixing in the Texaco Controlled Combustion Stratified Charge Engine," Fluid Mechanics Laboratory Report No. 76-1. January 1976.

7. Martin, M.K., "Photographic Study of Stratified Combustion Using a Rapid Compression Machine." S.M. Thesis, M.I.T., 1975.

8. Woschni, G., "A Universally Applicable Equation for the Instantaneous Heat Transfer Coefficient in the Internal Combustion Engine." SAE Paper 670931.

9. Blizard, N., and Keck, J.C., "Experimental and Theoretical Investigation of Turbulent Burning Model for Internal Combustion Engines." SAE Paper 740191.

10. Lazarewicz, M., "Performance of Texaco Startified Charge Engine on Gasoline." S.M. Thesis, M.I.T., 1975.

LIST OF SYMBOLS

The following symbols have been used throughout the text unless noted otherwise:

A_a	Wall area in contact with unburned gas mixture
A_b	Wall area in contact with the hot burned gas plume
A_{cup}	Surface area of the cup in the piston
A_T	Total wall area for heat transfer
b	Cylinder bore
C_p	Specific heat at constant pressure
C_v	Specific heat at constant volume
D	Effective valve diameter
d_c	Diameter of the cup in piston
E	Total internal energy
e	Specific internal energy
F_c	Chemically correct fuel to air ratio
$(G\text{-}F)_{S\text{-}P}$	Gas-to-fuel ratio at the spark plug
h	Specific enthalpy
L	Valve lift
LHV	Lower heating value of the fuel
m	Mass in the cylinder
m_{ex}	Cumulative mass flow through exhaust valve during exhaust phase
m_{fb}	Mass of fuel burned
m_{in}	Cumulative mass flow through intake valve during intake exhaust

MW	Molecular weight
$\dot{m}$	Mass rate of flow
$\dot{m}_e$	Mass rate of entrainment by the plume
N	Engine speed
P	Cylinder pressure
Q	Heat transfer to the walls
R	Specific gas constant
r	Characteristic plume radius
S	Stroke of the engine
S_e	Surface area of the plume for entrainment
T	Temperature
U_e	Eddy entrainment velocity
V	Total volume
v	Specific volume
V_{cup}	Volume of the cup in the piston
V_s	Swirl velocity
W	Work done by the charge
γ	Ratio of the specific heats
ρ	Density
ϕ	Equivalence ratio
ϕ_c	Equivalence ratio for combustion during rapid combustion phase
ϕ_o	Overall equivalence ratio

Subscripts

A	Air
b	Burned gas
cup	Cup in the piston
EGR	Exhaust gas recirculated
e	Entrainment
ex	Exhaust
in	Intake
O	Reference-at the end of intake phase or beginning of compression phase
RG	Residual gas
u	Unburned gas mixture
w	Engine walls

APPENDIX I

The Plume Geometry Model and Heat Transfer

During and after rapid combustion, the charge inside the cylinder consists of a plume of hot burned gas surrounded by an unburned gas mixture. Parts of the walls of the combustion chamber are in contact with the hot, burned gas plume and the remaining sections are in contact with relatively cold unburned gas mixture. The total heat transfer area can be divided into two parts and a plume geometry model is required to determine the two areas for heat transfer. In addition, the computations for the rate of entrainment of gas mixture by the plume during the mixing-dominated phase of combustion require knowledge of the surface area of the plume. The model for computing the plume geometry draws partly on the combustion movies taken on the Texaco engine. These high speed combustion movies were taken at a frequency of about 16,000 frames per second. During the initial phases of rapid combustion, the development of the plume can be clearly observed on the combustion movies and it appears that the plume starts at the spark plug and is swept around in the flow field induced by high swirl rates. After the initial phases, the intense radiation from the flames distorts the apparent plume geometry.

The Model

We assume that the plume starts at the spark plug and is swept around in swirling air flow. We assume that the plume grows in a uniform manner laterally around the spark-plug radius (R) until growth in any direction is impeded by the presence of chamber walls.

The contact with chamber walls in any direction is assumed to prevent further growth in that direction without affecting the rate of growth in any other direction.

The plume geometry model is then divided into three phases as shown in Figure (A-1);and Figure (A-2) is a schematic which defines all the symbols to be used in the model. During the first stage of combustion the burned gas plume does not touch any of the combustion chamber walls and all heat transfer areas are in contact with relatively cold unburned gas mixture. The plume is considered to be a section of a torus. As combustion proceeds, an ever increasing part of the total combustion chamber wall area comes in contact with the burned gas plume and the plume is assumed to consist of either two hollow discs on top of each other (Stage II) or two solid discs on top of each other (Stage III) as shown in Figure (A-1).

<u>Stage 1</u>: The boundaries of the three stages are defined in terms of the volume occupied by the burned gas plume. The first stage covers the initial development of the plume and ends when the cross sectional radius, r, of the torus becomes equal to ℓ, or at the time that the plume approaches the chamber walls. Thus, stage 1 covers the region when

$$0 \leq V_b \leq V_1 \tag{A1-1}$$

where

$$V_1 = 2\pi^2 \left(\frac{d_c}{2} - \ell\right)\ell^2$$

is the volume of a torus with inner radius $(\frac{d_c}{2} - 2\ell)$ and outer radius $\frac{d_c}{2}$.

The volume of the torus, in this stage, is given as

$$V_b = 2\pi^2(\frac{d_c}{2} - r)r^2 \tag{A1-2}$$

and r is the characteristic radius of the plume. During stage 1, all the walls of the chamber are in contact with unburned gas mixture so that

$$A_b = 0$$
$$A_a = A_t \tag{A1-3}$$

where

$$A_T = \frac{\pi b^2}{4} + \pi b\, x + \frac{\pi}{4}(b^2 - d_c^{\,2}) + A_{cup} \tag{A1-4}$$

The surface area of the plume is given by

$$S_e = 4\pi^2 Rr \tag{A1-5}$$

where

$$R = (\frac{d_c}{2} - \ell)$$

Stage II: The plume is assumed to consist of two hollow discs on top of each other (see Figure A1-1). This stage ends when the characteristic radius r of the plume equals R, so that Stage II covers the region

where

$$V_1 < V_b \leq V_2 \tag{A1-6}$$

where

$$V_2 = 4\pi\ x\ (\frac{d_c}{2} - \ell)^2 + \frac{\pi}{4}\ (\frac{d_c}{2} - x)\ d_c^{\ 2} \qquad \text{(A1-7)}$$

and the characteristic radius of the plume is obtained by recognizing that the volume during this stage is given by

$$V_b = 4\pi\ x\ Rr + \pi[(\ell-x) + r]\ [(\frac{d_c}{2})^2 - (R-r)^2] \qquad \text{(A1-8)}$$

The wall areas in contact with hot, burned gas plume and relatively cold gas mixture are:

$$A_b = 4\pi\ Rr + \pi d_c(r+\ell-x) + \pi[(R+r)^2 - (\frac{d_c}{2})^2] \qquad \text{(A1-9)}$$

$$A_a = A_T - A_b$$

where A_T is given by (A1-4).

The surface area of the plume for entrainment is given as

$$S_e = 2\pi(R+r)\ x + \pi(r+\ell)[3(R-r) + \frac{d_c}{2}] \qquad \text{(A1-10)}$$

<u>Stage III</u>: The plume is considered to consist of two solid discs on top of each other (see Figure A1-1) and this phase ends when the plume touches cylinder walls and the characteristic radius r equals (b/2-R). The period covered in this stage is given by

$$V_2 < V_b \leq V_3 \qquad \text{(A1-11)}$$

where

$$V_3 = \frac{\pi}{4}\ x\ b^2 + \frac{\pi}{4}[\frac{b}{2} - R + \ell - x]d_c^{\ 2}$$

and the characteristic radius of the plume, r, is obtained by the relationship

$$V_b = \pi x(R+r)^2 + \frac{\pi}{4}(r+\ell-x)d_c^{\,2} \qquad \text{(A1-12)}$$

The areas for heat transfer are

$$A_b = \pi(R+r)^2 + \pi[(R+r)^2 - (\frac{d_c}{2})^2] + \pi d_c(r+\ell-x) \qquad \text{(A1-13)}$$

and

$$A_a = A_T - A_b$$

where A_T is again given by (A1-4). The surface area of the plume for entrainment is given as

$$S_e = 2\pi(R+r)x + \frac{\pi d_c^{\,2}}{4} \qquad \text{(A1-14)}$$

At the end of the third . *period* the volume V_3 may not equal the instantaneous volume of the cylinder because of the cup in the piston.

Hence

for $V_3 < V_b < V$

$$A_b = (A_b)_3 + [A_t-(A_b)_3]\,[\frac{V_b-V_3}{V-V_3}]^{2/3} \qquad \text{(A1-15)}$$

$$A_a = A_T - A_b$$

and

$$S_e = (S_e)_3\,[\frac{V-V_b}{V-V_3}]^{2/3} \qquad \text{(A1-16)}$$

where $(A_b)_3$ and $(S_e)_3$ are the values of A_b and S_e at the end of Stage III

$$(A_b)_3 = \frac{\pi b^2}{4} + \frac{\pi}{4}(b^2 - d_c^{\ 2}) + \pi d_c\left(\frac{b}{2} - R + \ell - x\right) \tag{A1-17}$$

and

$$(S_e)_3 = \frac{\pi d_c^{\ 2}}{4} \tag{A1-18}$$

Plume geometry model is required only during rapid combustion and mixing - dominated phases since the plume and the unburned gas mixture co-exist only during this period. Before rapid combustion phase, the charge consists of unburned gas mixture alone while after the end of mixing dominated phase, the charge consists of burned gas only.

Heat Transfer Equation:

The heat transfer equation is given as:

$$Q = h_a A_a (T_a - T_w) + h_b A_b (T_b - T_w) \tag{A1-19}$$

where

$$h_a = 7014\ b^{-0.2} p^{0.8} T_a^{\ -0.53} \left[C_1\left(\frac{SN}{30}\right) + 100\, C_2 \frac{VT_o}{P_o V_o}(p - p_{is}) + (V_s)_a\right]^{0.8} \tag{A1-20}$$

and

$$h_b = 7014\ b^{-0.2} p^{0.8} T_b^{\ -0.53} \left[C_1\left(\frac{SN}{30}\right) + 100\, C_2 \frac{VT_o}{P_o V_o}(p - p_{is}) + (V_s)_b\right]^{0.8} \tag{A1-21}$$

TABLE 1

LIST OF INPUTS FOR PARAMETRIC ANALYSIS USING

THE PERFORMANCE MODEL

Present Values of the parameters at 2500 RPM, 45 mm^3 Fuel/Injection.

% Exhaust gas recirculated	= 0.
Injection timing (start)	= 25^oBTC
Gas-to-fuel ratio	= 10.6
Injection duration	$\simeq$ 32 CA^o

Range of Values for Parametric Study

Parameter	
% Exhaust gas recirculated	0, 5, 10, 15, 20
Injection timing, ^oBTC	45, 35, 25, 15, 5
Gas-to-fuel ratio at the spark plug	6, 8, 10.6, 13, 16
Injection Duration, CA^o	10, 20, 30, 40, 50

[A square wave injection profile assumed]

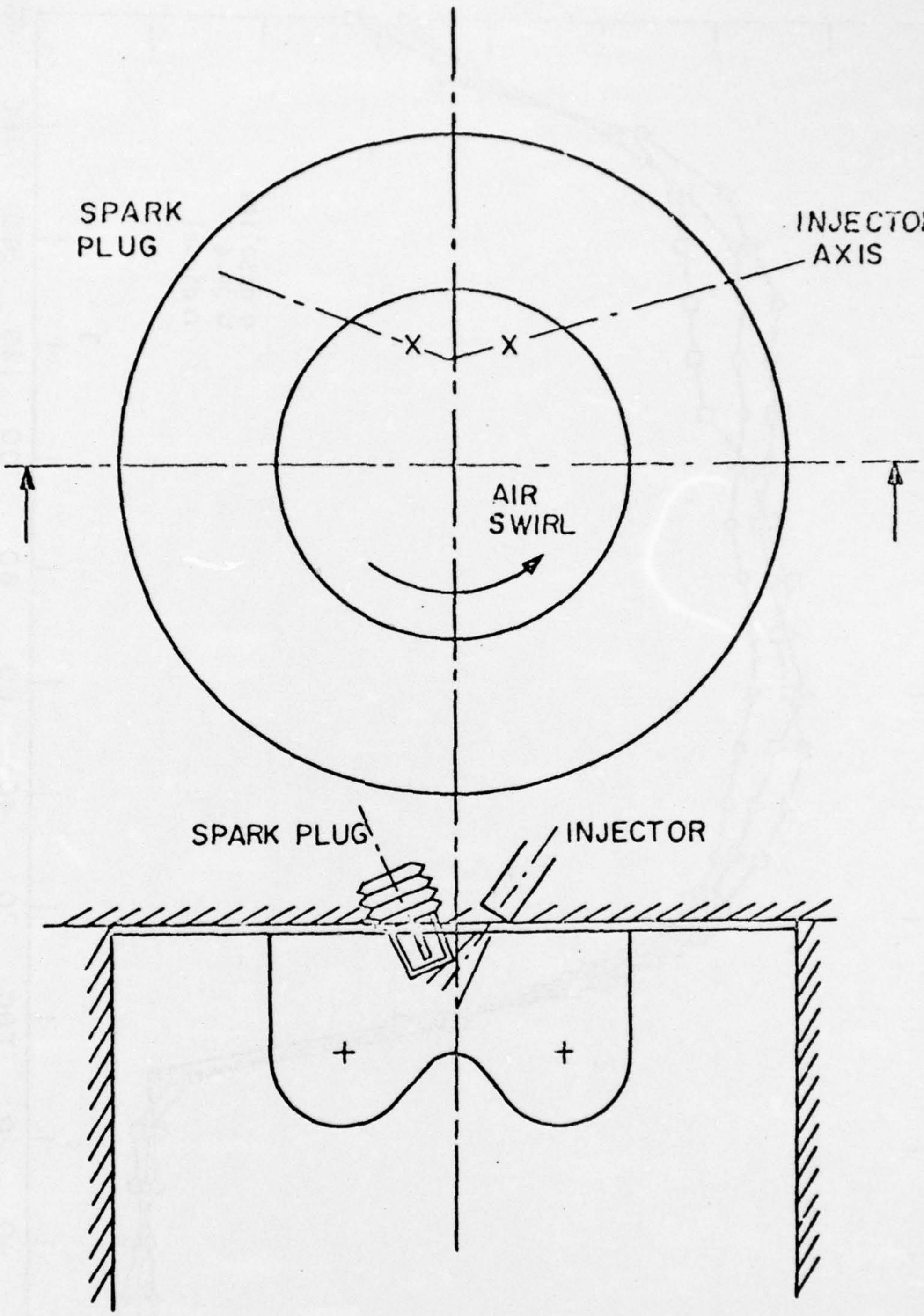

TEXACO CONTROLLED COMBUSTION
SYSTEM (SCHEMATIC)

Figure 1

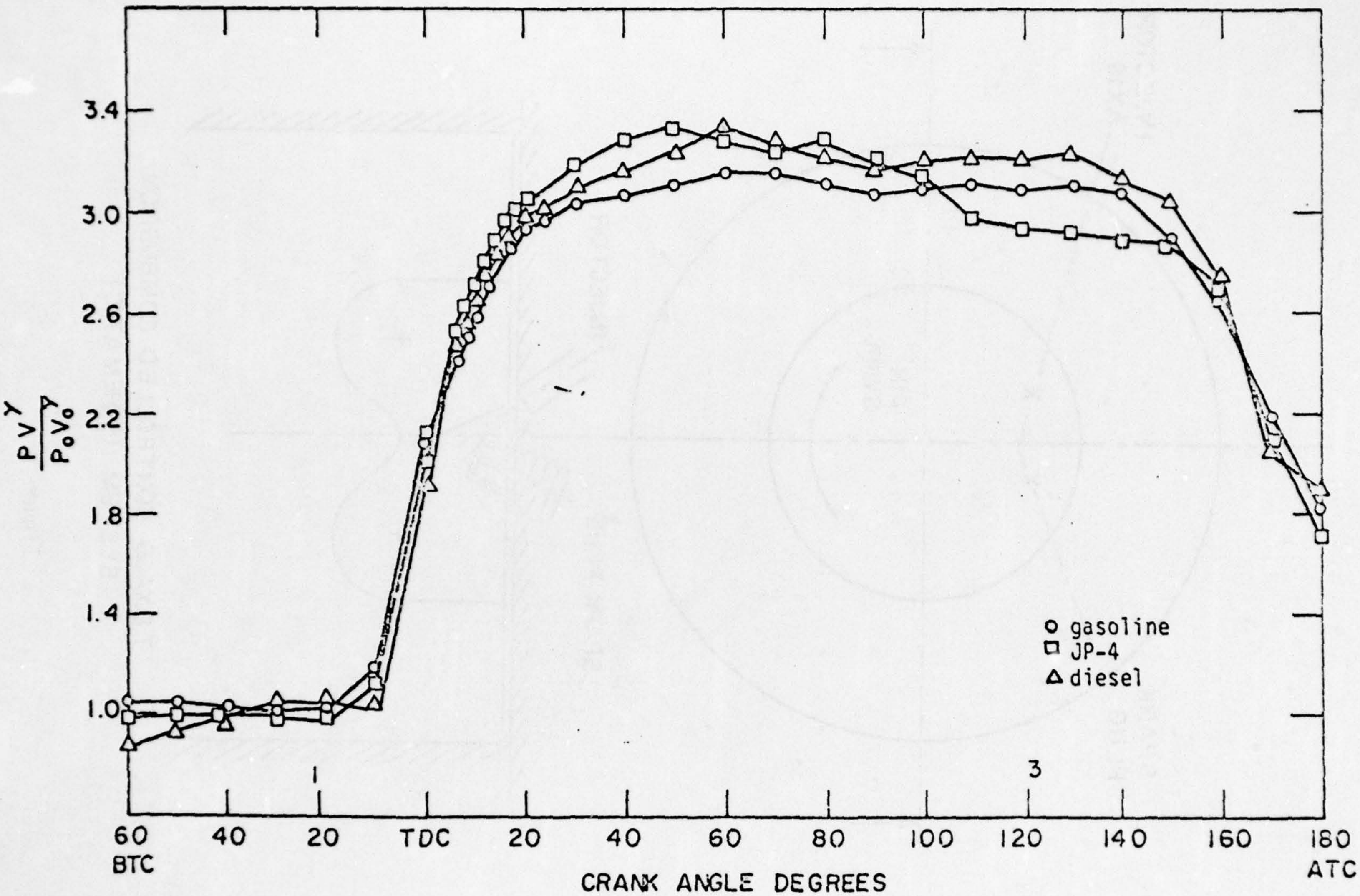

Figure 2 PV^{γ} plot using experimental data on HCC engine - 1200 RPM, full load

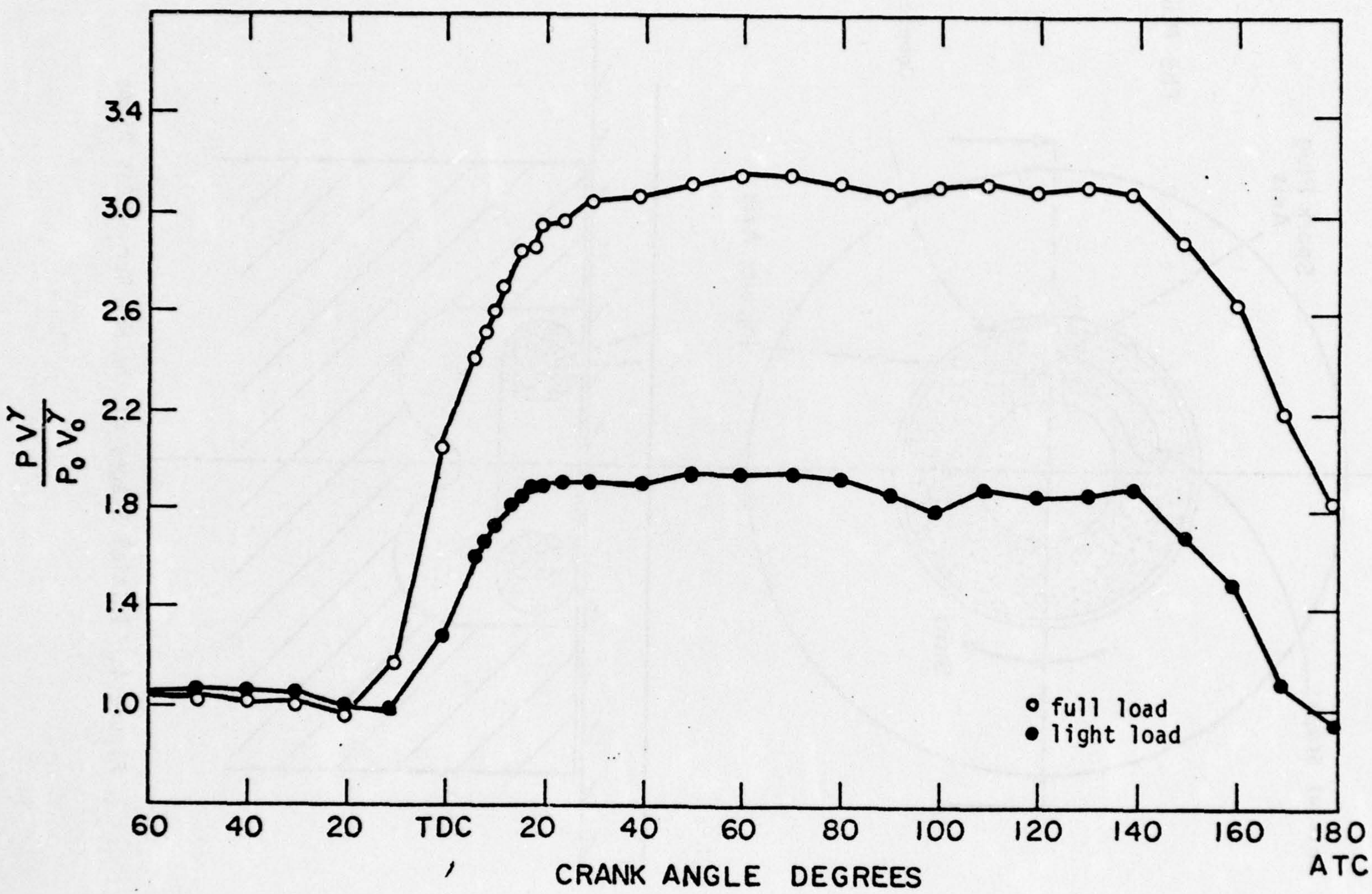

Figure 3: PV plot using experimental data on HCC engine - 1200 RPM, gasoline

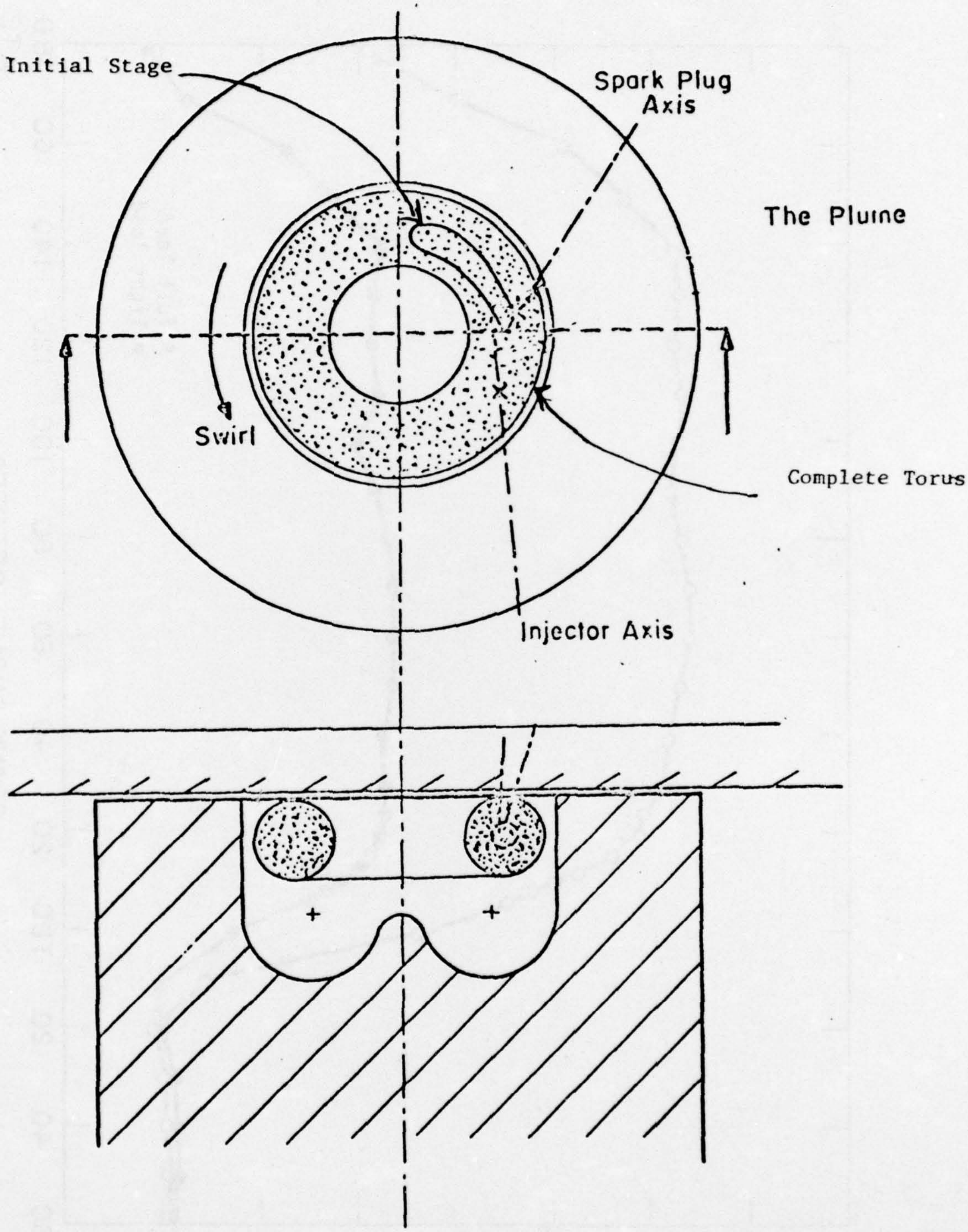

Figure 4: Initial Stages of the Hot Burned Gas Plume

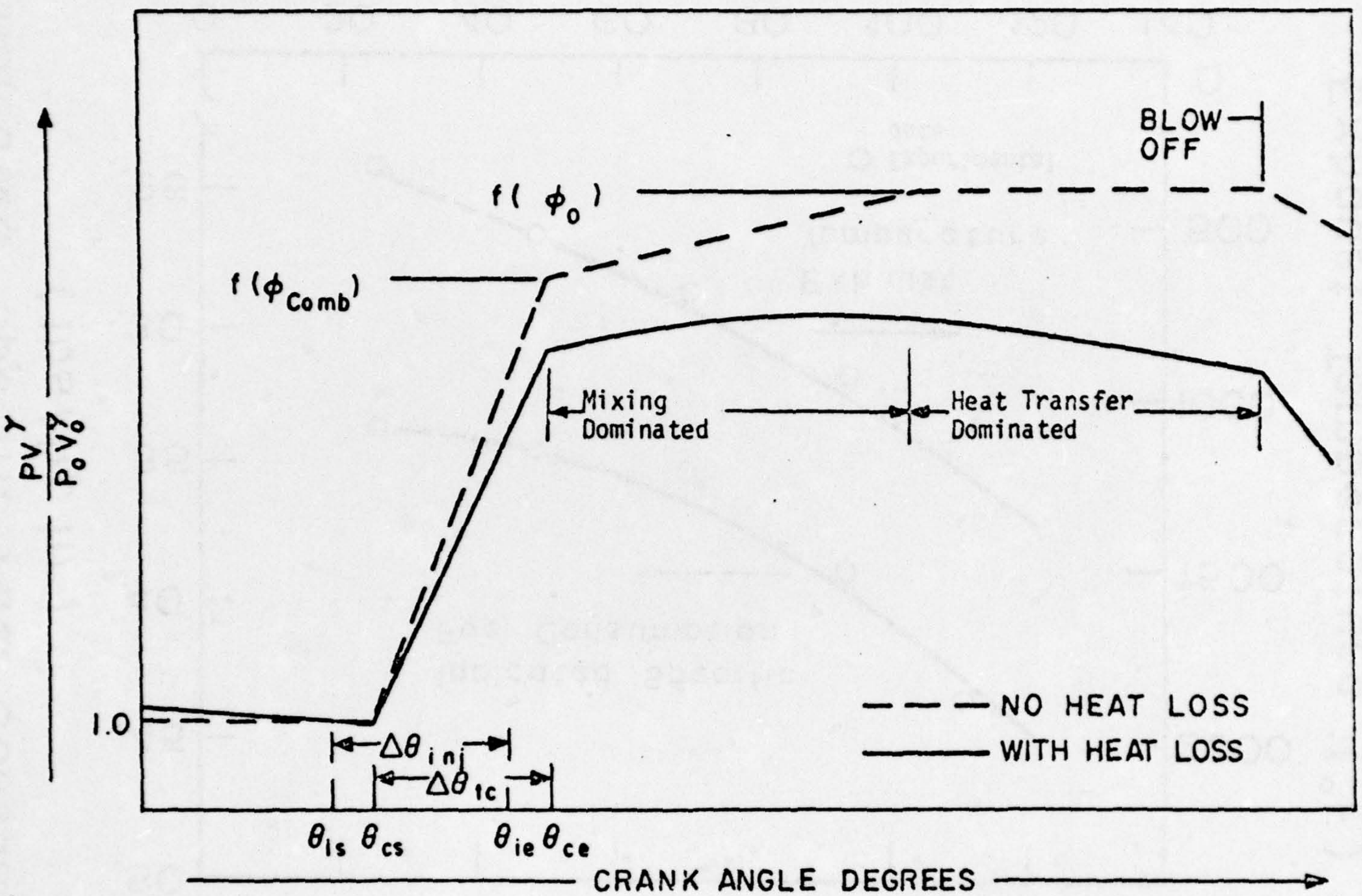

Figure 5 Simplified PV^{γ} plot (Theory). $\Delta\theta_{inj}$ and $\Delta\theta_{rc}$ are injection and rapid combustion durations respectively.

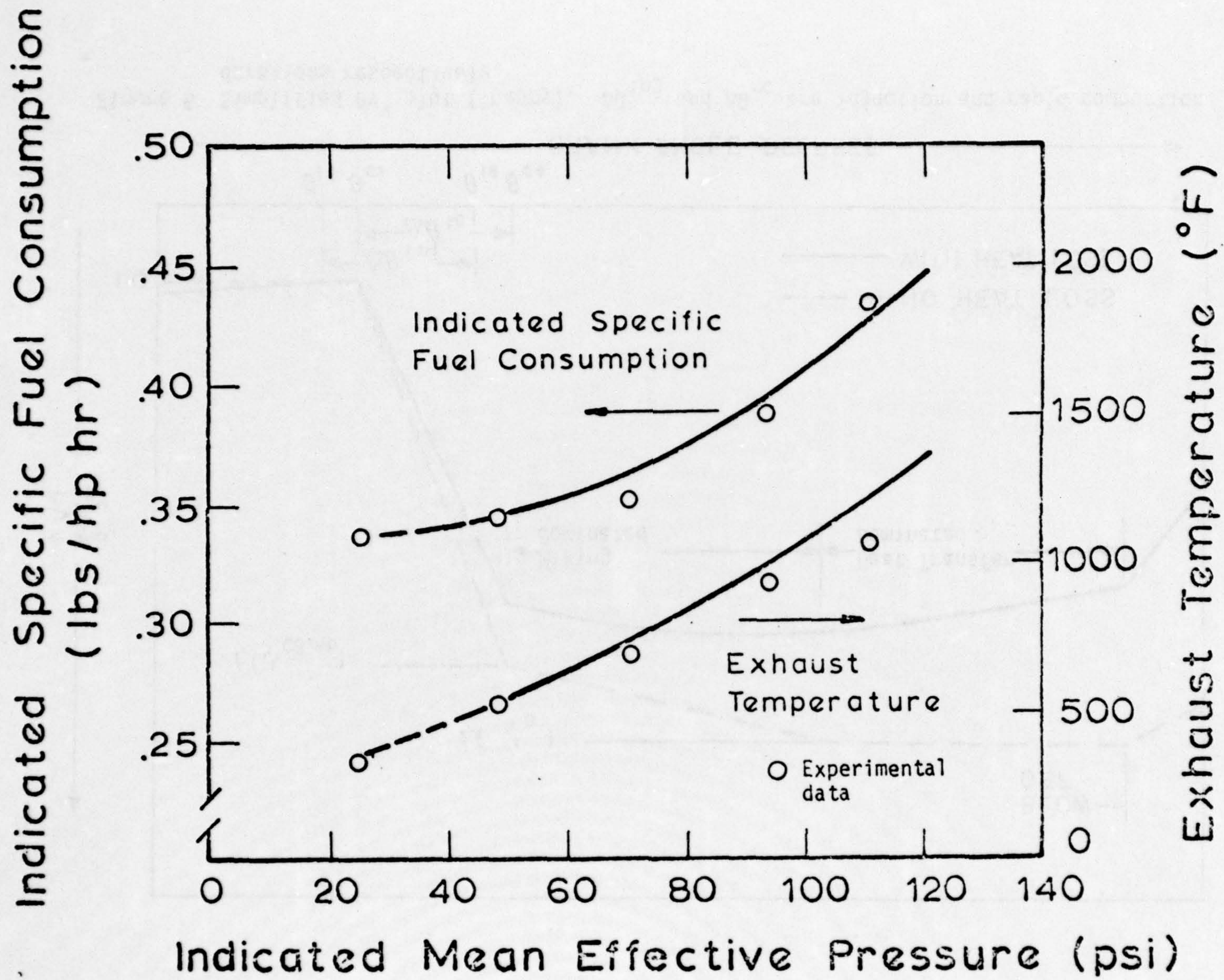

Figure 6: Predictions of the model compared with experimental data - 1500 RPM

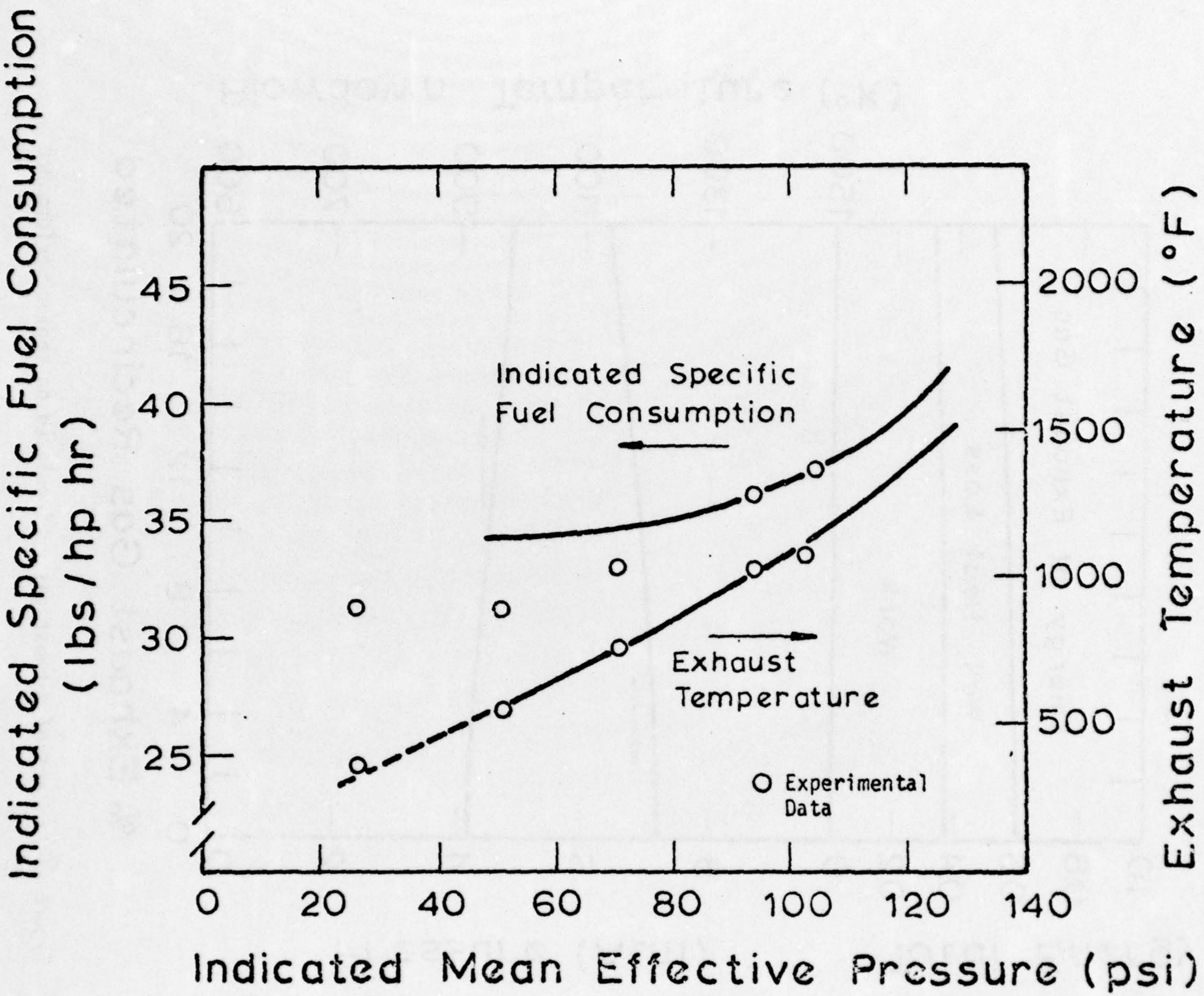

Figure 7: Predictions of the model compared with experimental data - 2500 RPM

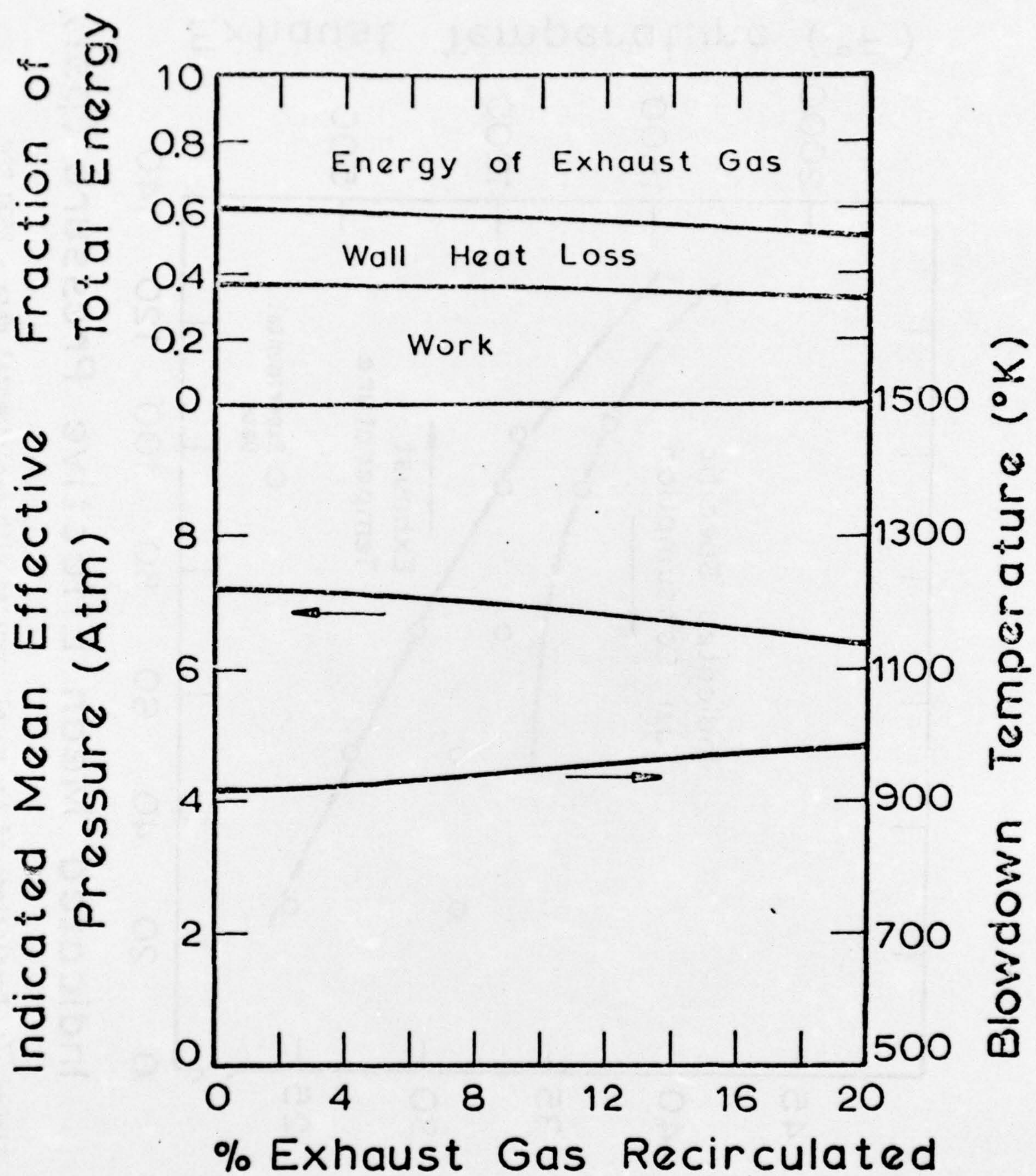

Figure 8: Effect of exhaust gas recirculated on engine performance

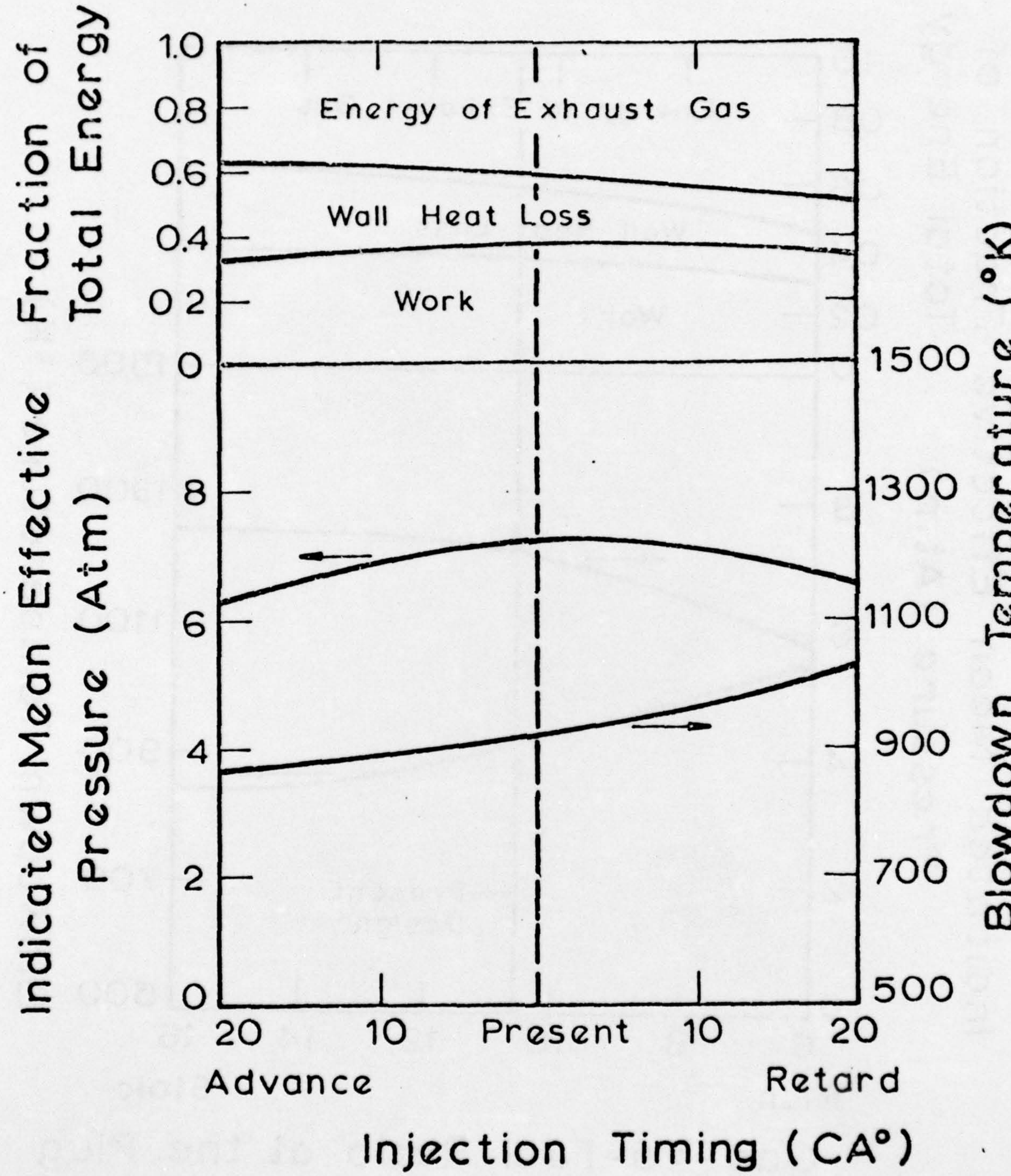

Figure 9: Effect of injection timing on engine performance

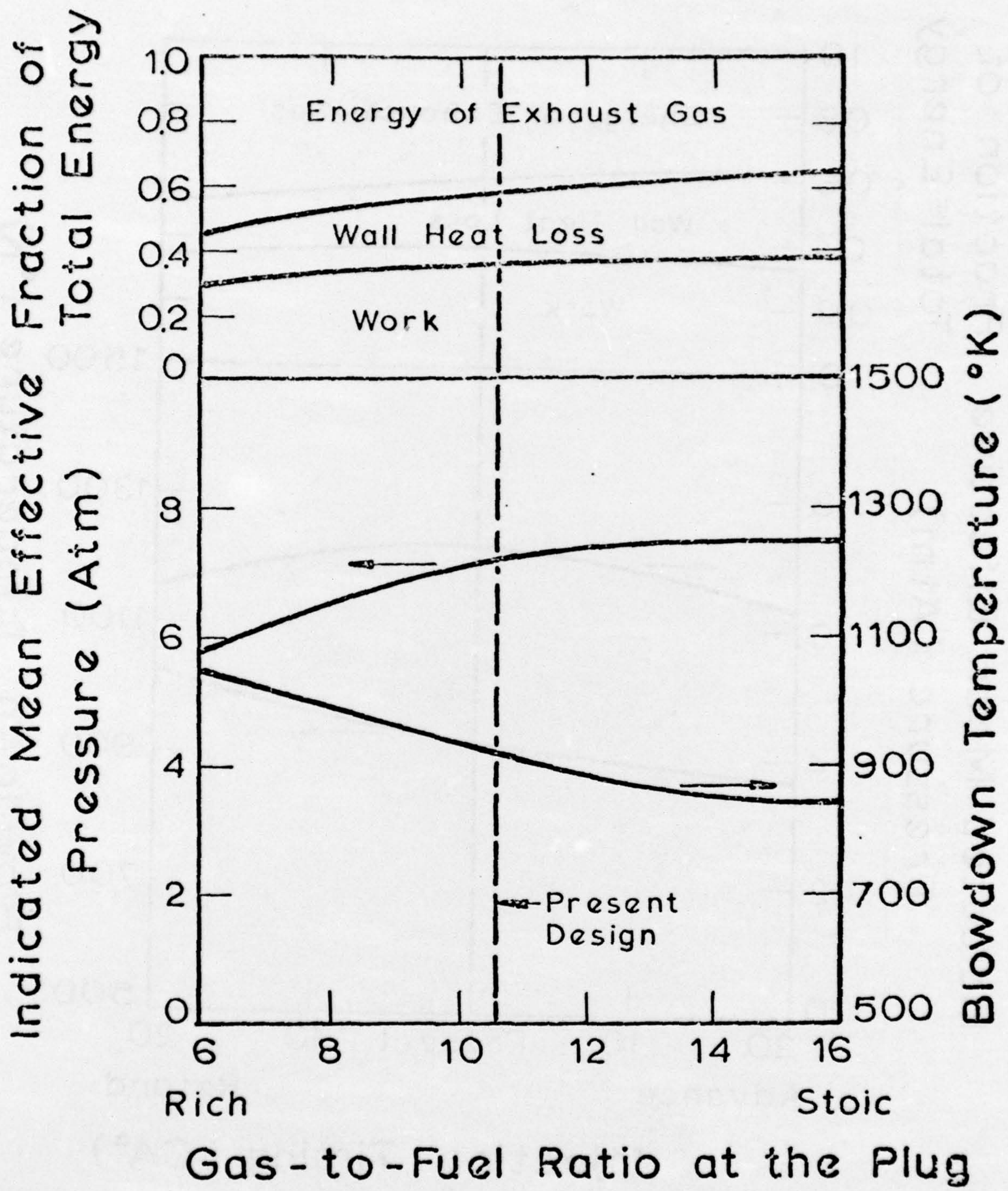

Figure 10: Effect of gas-to-fuel ratio on engine performance

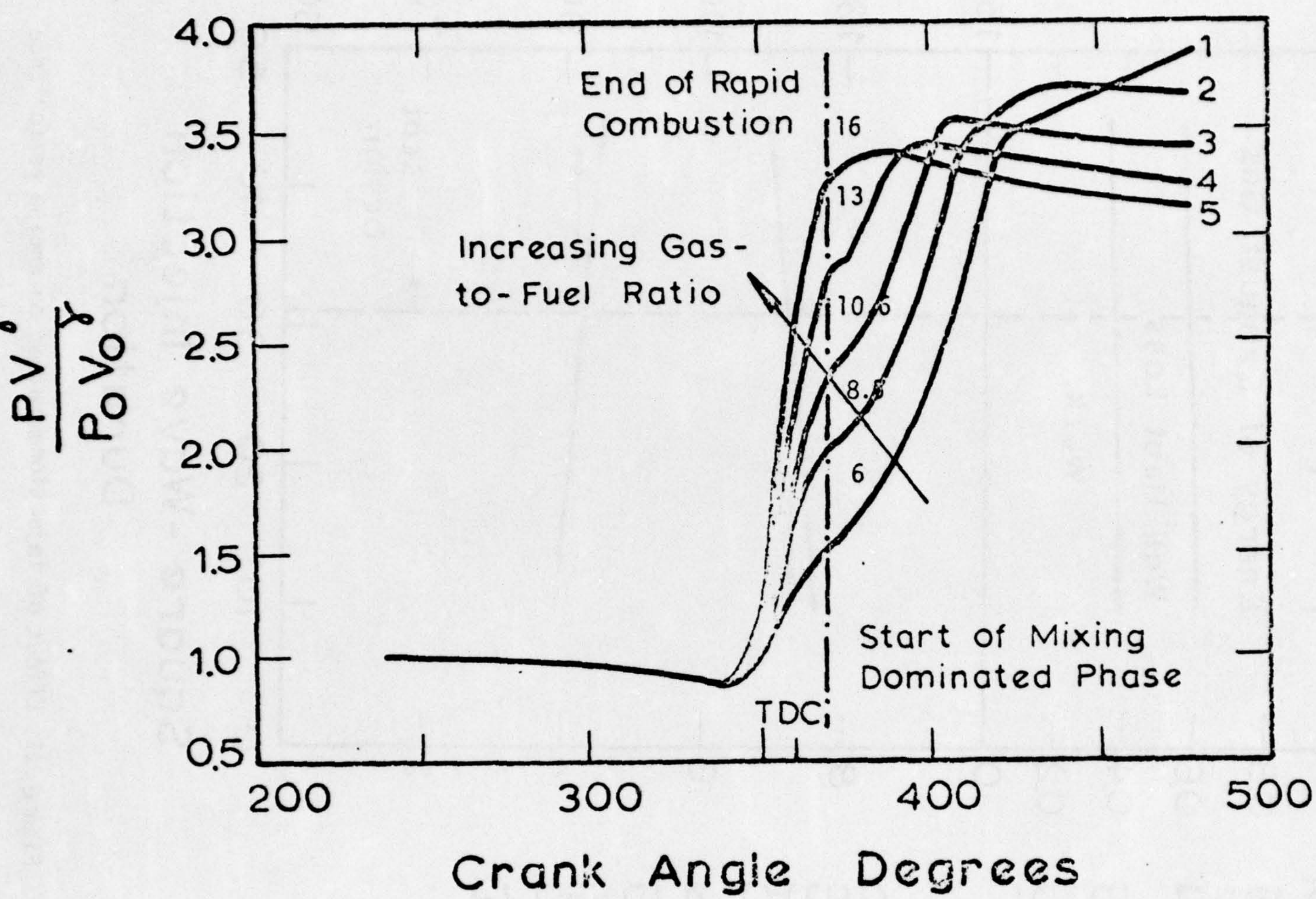

Figure 11 Effect of gas-to-fuel ratio at the plug on PV^{γ}

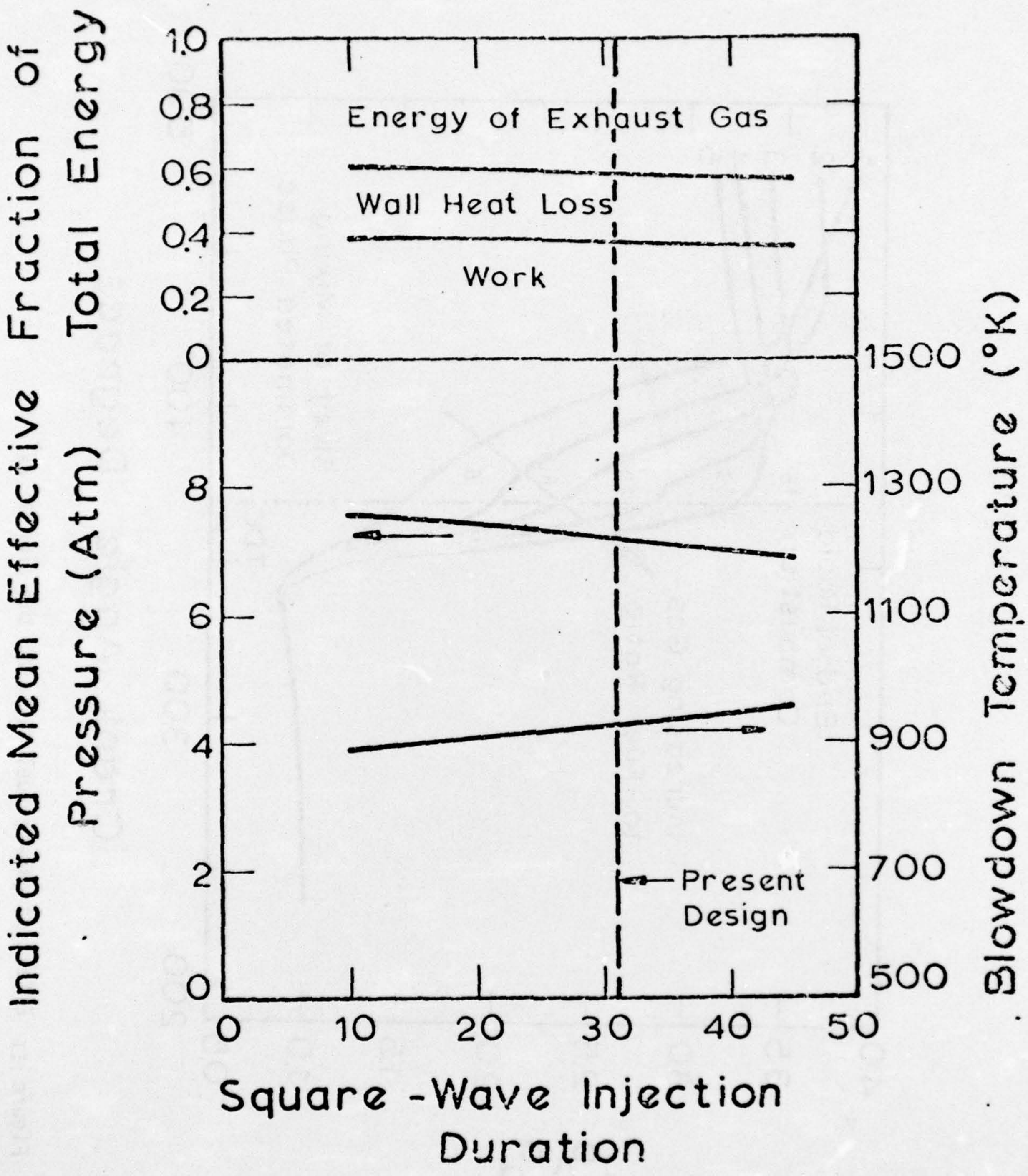

Figure 12 Effect of injection duration on engine performance

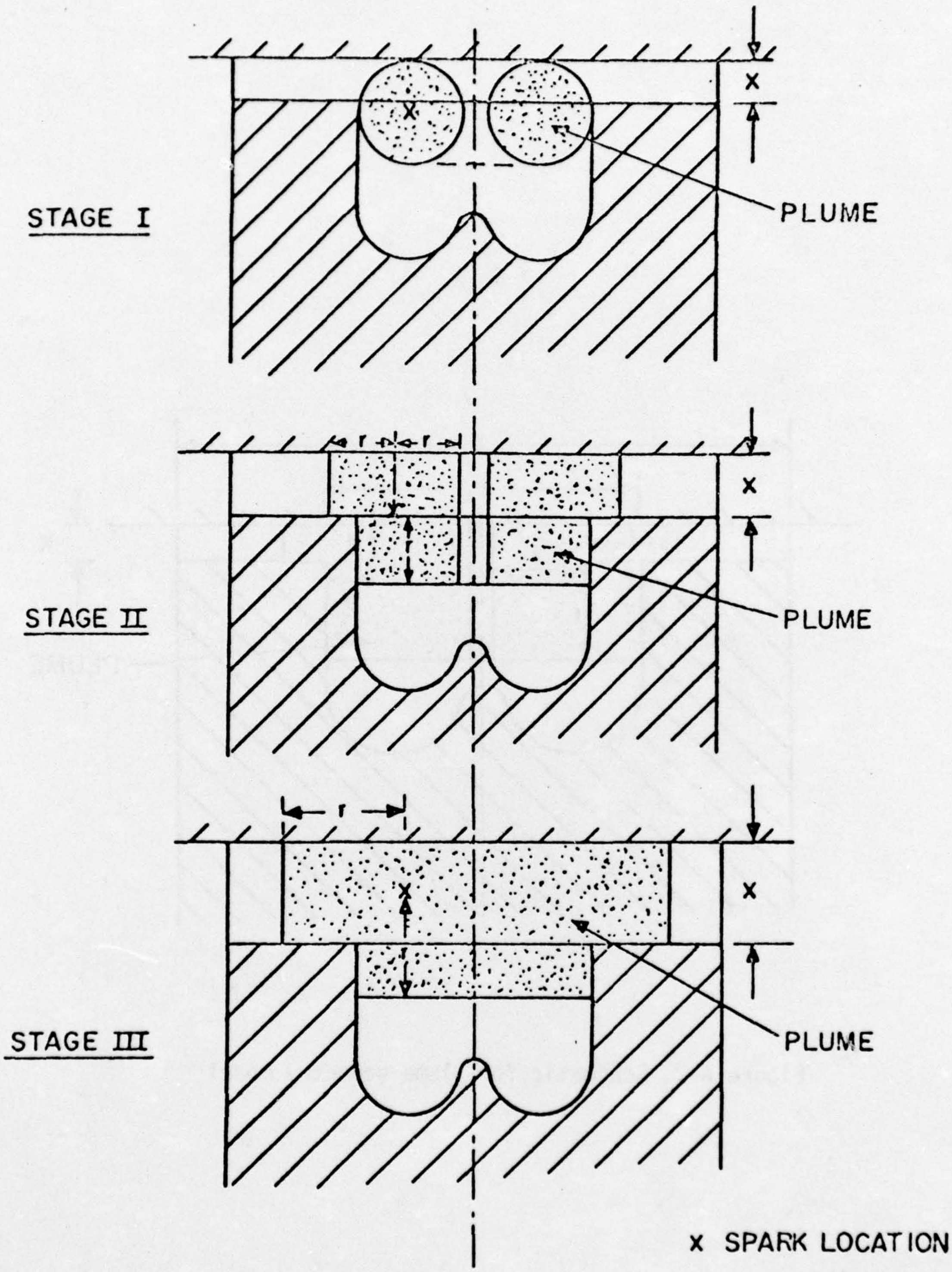

Figure A-1 Various stages in the plume geometry model

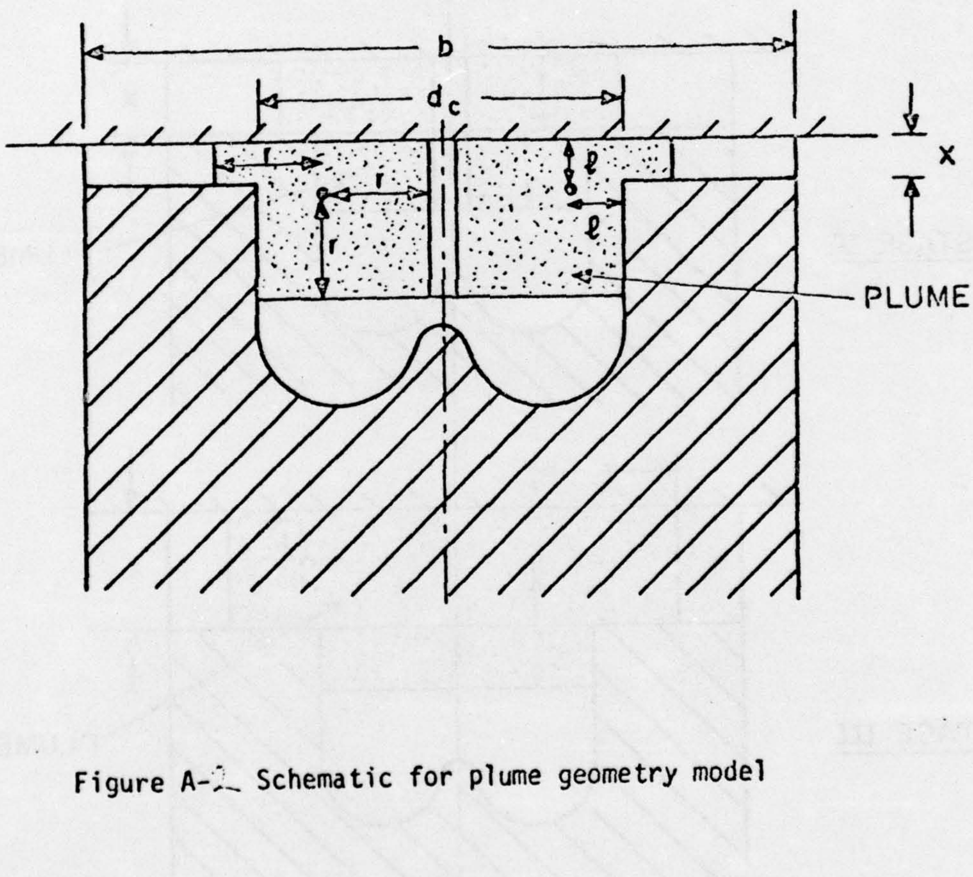

Figure A-2 Schematic for plume geometry model